




Osteoid osteoma of the rib with strong F-18 fluoro-deoxyglucose uptake mimicking osteoblastoma: a case report with literature review

Acta Radiologica Open
10(6) 1–5
© The Foundation Acta
Radiologica 2021
Article reuse guidelines:
sagepub.com/journals-permissions
DOI: 10.1177/20584601211022497
journals.sagepub.com/home/arr


Yuka Ishikura¹ , Rika Yoshida¹, Takeshi Yoshizako¹ ,
Kouji Kishimoto², Noriyoshi Ishikawa^{3,4}, Riruke Maruyama³ and
Hajime Kitagaki¹

Abstract

Osteoid osteoma is a benign osteoblastic bone lesion, characterized by nocturnal pain alleviated by salicylates or nonsteroidal anti-inflammatory drugs. This tumor distinctly affects the long bones, typically the femur or tibia and is rarely located in the ribs. Usually, this tumor is usually diagnosed by computed tomography or magnetic resonance imaging, but F-18 fluoro-deoxyglucose positron emission tomographic (FDG-PET)/computed tomography is usually negative and is not used for diagnosis. We recently encountered a case of an osteoid osteoma located in the rib of 44-year-old Asian male with strong FDG uptake as high as 12.0 at the maximum standardized uptake value at FDG-PET/computed tomography. His computed tomography and magnetic resonance imaging showed osteosclerosis, bone marrow edema, and edema of surrounding tissues not only in the bone with nidus but also in the adjacent bone, and pathological findings showed strong infiltration mimicking radiology. Strong FDG uptake mimicking osteoblastoma. Osteoid osteoma with strong FDG uptake suggested a strong inflammatory response.

Keywords

Osteoid osteoma, osteosclerosis, FDG, positron emission tomographic, magnetic resonance imaging, computed tomography

Received 28 February 2021; accepted 17 May 2021

Introduction

Osteoid osteoma (OO) is a painful, osteoblastic bone lesion, benign in nature, and which could be described as a nidus of osteoid tissue (unmineralized bone matrix). OO contributes to 10% of all benign bone tumors. This tumor is mostly seen between the ages of 7 and 25 years and has a predilection toward males.¹ OO is characteristically known for nocturnal pain that is relieved by salicylates or nonsteroidal anti-inflammatory drugs (NSAIDs).² OO distinctly affects the long bones, typically the femur or tibia and is rarely located in the ribs. Less than 1% of all OO are found in the ribs and several cases of rib OO are currently published in the literature.³ OO is usually diagnosed using computed tomography (CT) or magnetic resonance imaging (MRI). F-18

fluoro-deoxyglucose positron emission tomographic (FDG-PET)/CT is usually used to distinguish OO from malignant bone tumors as it is usually FDG-negative. Herein, we present a case of rib OO with

¹Department of Radiology, Faculty of Medicine, Shimane University, Shimane, Japan

²Department of Respiratory Surgery, Faculty of Medicine, Shimane University, Shimane, Japan

³Department of Organ Pathology, Faculty of Medicine, Shimane University, Shimane, Japan

⁴Department of Pathology, Faculty of Medicine, Shonan Fujisawa Tokushukai Hospital, Fujisawa, Japan

Corresponding author:

Yuka Ishikura, Department of Radiology, Faculty of Medicine, Shimane University, 89-1, Enya-cho, Izumo, Shimane 693-8501, Japan.
Email: es_yama921@yahoo.co.jp



strong FDG uptake and osteosclerosis of not only the affected rib but also the surrounding ribs.

Case report

A 44-year-old Asian male patient presented with a two-year history of pain in the medial part of his left scapula. An abnormality in the shadow of the fourth right side was seen on a chest radiograph (Fig. 1). CT scan showed a 10-mm-sized circular translucent lesion in the right fourth rib. The lesion contained an intracortical calcified nidus surrounded by osteosclerosis. In addition, the osteosclerotic change was predominantly seen in the dorsal/ventral side of the fourth rib and of the surrounding ribs (Fig. 2(b), arrows).

Blood tests showed slightly high values of CEA 5.5 ng/ml (normal range: <5.0 ng/mL). MRI and F-18 FDG-PET/CT scan were performed to rule out malignant diseases, including metastatic tumors. MRI showed nonuniform high signal on fat-suppression T2-weighted image (T2WI) (Fig. 3(a), arrow) and low signal on T1WI (Fig. 3(b)). The surrounding soft tissue showed a low signal at T1WI and a high signal at T2WI, suggesting edematous changes. Fat-suppression T2WI showed bone marrow edema in the fourth rib that had lesions, and bone marrow edema on the upper and lower adjacent ribs (Fig. 3(c)). PET/CT scan also showed FDG uptake within the nidus, and the SUV max (maximum standardized uptake value) was as strong as 12.0 (Fig. 4). No significant accumulation was found in the curability changes around the nidus.

Following this, a partial resection of right fourth rib was performed for diagnostic and analgesic purposes. Surgical specimens (Fig. 5(a)) showed a round lesion of a little over 1 cm, consistent with the nidus on CT. On pathological examination, the nidus had patchy osteosclerotic lesions and irregular anastomotic calcified trabeculae, surrounded by swollen osteoblasts without atypical cell (Fig. 5(b)). Based on these findings, the diagnosis of OO was made. Over than the above, the inflammatory cells and mesenchymal cells were seen around the fourth intercostal muscle and the parietal pleura, in a state that involved the adipose tissue and skeletal muscles accompanied by edematous fibrosis (Fig. 5(c)).

After treatment, the patient was doing well and was discharged. There was no recurrence of symptoms at the 18-month follow-up examination.

Discussion

Imaging findings of OO show thickening and hardening of cortical bone on plain X-rays, showing a nidus with a diameter of several mm to 1 cm, and circular to



Fig. 1. Chest X-ray. Increased concentration is observed in the right fourth rib (arrow).

oval, uncalcified transparent images. In the center, the old part may be calcified and recognized as a hardened image. X-ray even if it is not clear, CT makes it easier to detect a nidus.⁴ The MRI appearance of OO is variable, commonly exhibiting low to intermediate signal intensity on T1WI and heterogeneous high signal intensity on T2WI and fat-suppression T2WI.⁵⁻⁷ Perilesional sclerosis is seen as fusiform low signal with both T1WI and T2WI. MRI typically shows an intense surrounding bone marrow and soft tissue edema.⁸

In this case, the CT and MRI were consistent with the above findings and were typical imaging findings. We suspected OO first, although raising differential diseases (osteomyelitis, Langerhans cell histiocytosis, and bone metastasis). The diagnosis was not difficult, but there were two peculiar and characteristic findings, that is, it showed a high FDG uptake and caused osteosclerosis in the nearby ribs.

Osteoblastoma is a similar disease to OO, and both are pathologically identical and difficult to distinguish. Osteoblastoma typically has a lesion size of 1–2 cm or larger, with inconspicuous surrounding osteosclerosis and a weak effect of NSAIDs on pain.⁹ In this case, the size was 1 cm, which is relatively large for OO, but osteosclerosis was conspicuous, and NSAIDs reduced pain, so OO was diagnosed.

FDG is not the recommended PET tracer because OO is normally FDG-negative, although some OOs may show increased FDG uptake. Three cases of OO with FDG uptake were found, FDG uptake was about SUV max 4–9.^{10,11} In this case, SUV max was as high as 12, but there was no report showing stronger FDG

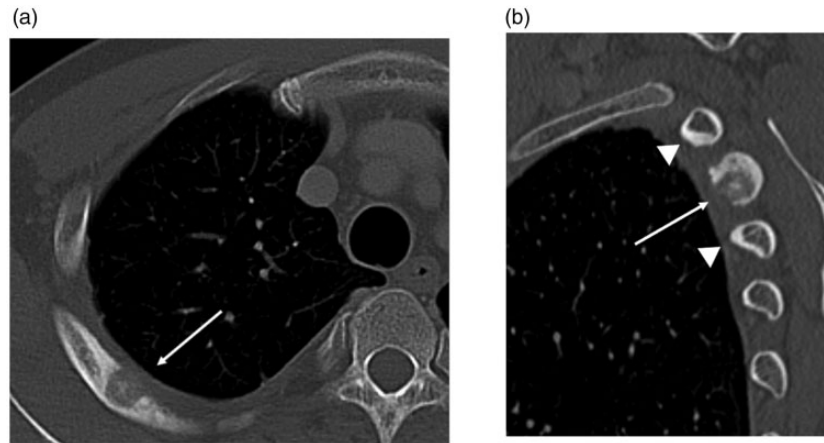


Fig 2. Noncontrast-enhanced CT scans. (a) Noncontrast-enhanced CT scan (Bone condition, window level (WL) = 500 Hounsfield Unit (HU), window width (WW) = 2500 HU), axial image. (b) Noncontrast-enhanced CT scan (Bone condition, WL=500 HU, WW=2500 HU), sagittal image. CT scan showed a 10-mm-sized circular bone translucent image is observed on the right fourth rib, with small calcification inside (a, arrow). The lesion contained an intracortical calcified nidus and was surrounded by sclerosis. A sclerotic change is observed in the surrounding bone (b, arrowhead), and an increase in the surrounding soft tissue concentration and the pleural thickening are observed.

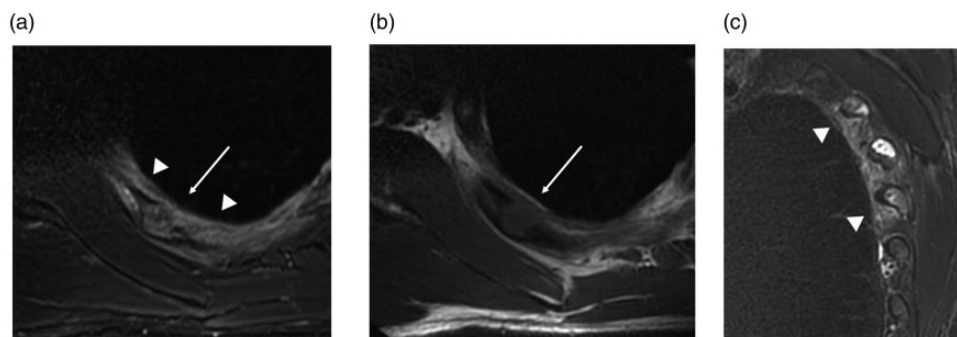


Fig 3. Magnetic resonance imaging. (a) Fat-suppression T2WI, axial image (Repetition Time (TR)=3000 ms, Echo Time (TE)=89 ms). (b) T1WI, axial image (TR=534 ms, TE=12.5 ms). (c) Fat-suppression T2WI, Sagittal image (TR=9592 ms, TE=100.4 ms). MRI showed non-uniform high signal on fat-suppression T2WI (a, arrow) and low signal on T1WI (b, arrow). The surrounding soft tissue showed a low signal at T1WI and a high signal at T2WI, suggesting edematous changes. Fat-suppression T2WI showed bone marrow edema on the fourth rib with lesions, and bone marrow edema on the upper and lower ribs (c, arrowhead).

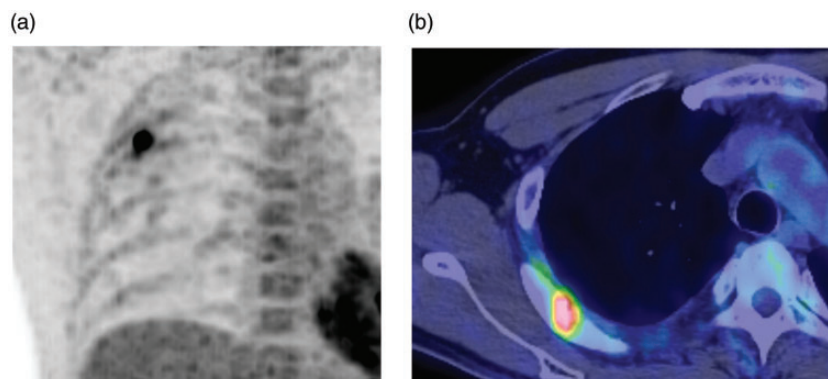


Fig 4. FDG-PET/CT. (a) Maximum intensity projection (MIP) image. (b) PET/CT fusion image. Combined FDG PET/CT was performed on a 16-multi-detector row CT (MDCT) scanner (Biograph 6 PET/CT, Emotion 16 CT, Siemens). Approximately 270 MBq of 18-F-FDG was administered intravenously as a bolus, and imaging was performed 60 minutes later. FDG-PET showed a strong FDG uptake as SUV max 12.0.

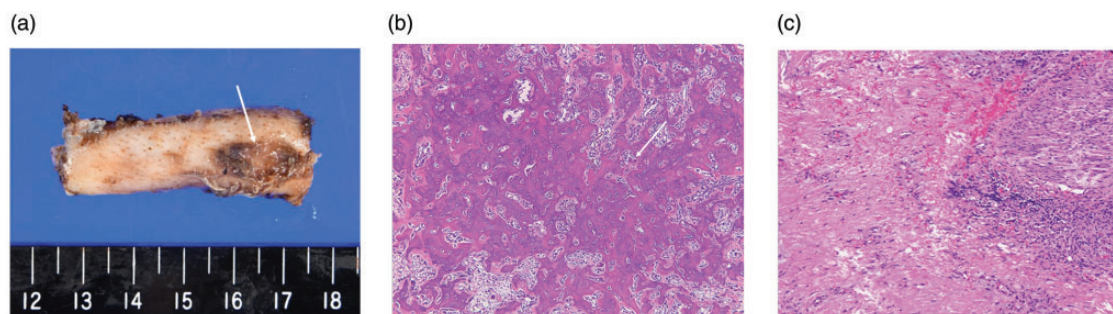


Fig 5. Pathological examination. (a) Surgical specimen. (b) Nidus, hematoxylin and eosin stain $\times 20$. (c) Parietal pleura, hematoxylin and eosin stain $\times 20$. Surgical specimens (a) show a round lesion of a little over 1 cm that is visually demarcated (a, arrow), consistent with nidus on CT. The center shows patchy osteosclerotic lesions and irregular anastomotic trabeculae with calcification, surrounded by swollen osteoblasts (b, arrow). The parietal pleura with the fourth rib had inflammatory cells and mesenchymal cells and a lot of fibrin fiber (c).

accumulation than this case. It currently remains unclear, which cells are responsible for FDG uptake in OO since autoradiography studies have not yet been performed. Since osteoblasts and activated inflammatory cells are present in OO, both could be the reason for positive FDG imaging. FDG uptake may correlate with pain or “activity” of OOs. In this case, it is presumed that there was more active inflammation than the normal OO.

In addition, unusually in this case, osteosclerosis was observed not only in the bone with a nidus but also in the surrounding tissues. To the best of our knowledge, there are some reports of rib OO in the literature; however, we were unable to find a report of OO of the rib with osteosclerosis of the surrounding bone. Only one case of OO in the metatarsal bone reported osteosclerosis in the bone adjacent to the affected metatarsal bone similar to what was observed in our case.¹² Although it is well known that osteosclerosis is present around a nidus in OO, there is limited focus on the mechanism of osteosclerosis. In OO, the nidus produces prostaglandin E2 (PGE2), which is not produced by the surrounding bone tissue, and this substance is responsible for the bone pain.¹³ PGE2 is known to induce significant increase in bone formation, bone mass, and bone strength when administered systemically or locally within the skeleton.^{14–16} It is possible that PGE2 produced from the nidus diffused to the surrounding tissue causing osteosclerosis of the adjacent cortical bone, inflammation in the surrounding soft tissue and thickening of the cortical bone adjacent to the lesion like in our case. In support of the above, pathological findings showed infiltration of mesenchymal cells and inflammatory cells in the surrounding tissues to involve adipose tissue and skeletal muscle, and the pleural membrane was also strongly fibrotic. There was infiltration of inflammatory cells

and infiltration of mesenchymal cells. From the above, a strong pathologically inflammatory reaction was suggested.

In this case, FDG-PET/CT also showed strong uptake in the nidus. Radiographic images and histopathological images showed a widespread inflammatory response. As the reason for admitting strong FDG uptake at FDG-PET/CT, we suspect strong inflammation, and the production of PGE2 in a larger amount than usual was considered as the background.

In conclusion, we presented a case of OO of the rib with strong FDG uptake mimicking malignancy, suggested a strong inflammatory response.

Acknowledgements

We thank Enago (www.enago.com) for the English language review.

Declaration of Conflicting Interests

The author(s) declared no potential conflicts of interest with respect to the research, authorship, and/or publication of this article.

Funding

This research did not receive any specific grant from funding agencies in the public, commercial, or not-for-profit sectors.

Informed consent

This case report has obtained Institutional Review Board approval and the formal informed consent from this patient was waived. We had obtained informed patient consent about all procedures.

ORCID iDs

Yuka Ishikura  <https://orcid.org/0000-0001-9432-9322>
Takeshi Yoshizako  <https://orcid.org/0000-0003-1623-1375>

References

1. Gökalp MA, Gözen A, Ünsal SŞ, et al. An alternative surgical method for treatment of osteoid osteoma: *Med Sci Monit* 2016;22:580.
2. Greenspan A. Benign bone-forming lesions: osteoma, osteoid osteoma, and osteoblastoma. *Skelet Radiol* 1993;22:485–500.
3. Unni KK. Dahlin's bone tumors: general aspects and data on 10,165 cases. Philadelphia, PA: LWW, 2010.
4. Noordin S, Allana S, Hilal K, et al. Osteoid osteoma: contemporary management. *Orthop Rev* 2018;10:3.
5. Papathanassiou ZG, Megas P, Petsas T, et al. Osteoid osteoma: diagnosis and treatment. *Orthopedics* 2008;31:11.
6. Assoun J, Richardi G, Railhac JJ, et al. Osteoid osteoma: MR imaging versus CT. *Radiology* 1994;191:217–223.
7. Davies M, Cassar-Pullicino VN, Davies AM, et al. The diagnostic accuracy of MR imaging in osteoid osteoma. *Skelet Radiol* 2002;31:559–569.
8. Bhure U, Justus E, Strobel K. Osteoid osteoma: multi-modality imaging with focus on hybrid imaging. *Eur J Nucl Med Mol Imaging* 2019;46:1019–1036.
9. Atesok KI, Alman BA, Schemitsch EH, et al. Osteoid osteoma and osteoblastoma. *J Am Acad Orthop Surg* 2011;19:678–689.
10. Lim CH, Park YH, Lee SY, et al. F-18 FDG uptake in the nidus of an osteoid osteoma. *Clin Nucl Med* 2007;32:628–630.
11. Imperiale A, Moser T, Ben-Sellem D, et al. Osteoblastoma and osteoid osteoma: morphofunctional characterization by MRI and dynamic F-18 FDG PET/CT before and after radiofrequency ablation. *Clin Nucl Med* 2009;34:184–188.
12. Kojiro O, Kiyoshi O, Hiroki S, et al. A case of osteoid osteoma in the left third metatarsal bone. *Orthop Traumatol* 2016;65: 66–70 (in Japanese).
13. Ciabattini G, Tamburrelli F, Greco F. Increased prostacyclin biosynthesis in patients with osteoid osteoma. *Eicosanoids* 1991;4:165–167.
14. Jee WSS, Ma YF. The in vivo anabolic actions of prostaglandins in bone. *Bone* 1997;21:297–304.
15. Ke HZ, Shen VW, Qi H, et al. Prostaglandin E2 increases bone strength in intact rats and in ovariectomized rats with established osteopenia. *Bone* 1998;23:249–255.
16. Yang RS, Liu TK, Lin-Shiau SY. Increased bone growth by local prostaglandin E 2 in rats. *Calcif Tissue Int* 1993;52:57–61.